Highly correlated ab initio study of the far infrared spectra of methyl acetate

M. L. Senent, R. Domínguez-Gómez, M. Carvajal, and I. Kleiner

Citation: J. Chem. Phys. **138**, 044319 (2013); doi: 10.1063/1.4789413
View online: http://dx.doi.org/10.1063/1.4789413
View Table of Contents: http://jcp.aip.org/resource/1/JCPSA6/v138/i4
Published by the American Institute of Physics.

Highly correlated *ab initio* study of the far infrared spectra of methyl acetate

M. L. Senent,[1,a)] R. Domínguez-Gómez,[2,b)] M. Carvajal,[3,c)] and I. Kleiner[4,d)]
[1]*Departamento de Química y Física Teóricas, Instituto de Estructura de la Materia, C.S.I.C., Serrano 121, Madrid 28006, Spain*
[2]*Doctora Vinculada al IEM-CSIC, Departamento de Ingeniería Civil, Cátedra de Química, E.U.I.T. Obras Públicas, Universidad Politécnica de Madrid, 28040 Madrid, Spain*
[3]*Unidad Asociada IEM-CSIC-Departamento de Física Aplicada, Facultad de Ciencias Experimentales, Universidad de Huelva, 21071 Huelva, Spain*
[4]*Laboratoire Interuniversitaire des Systèmes Atmosphériques (LISA), CNRS, UMR 7583, Université de Paris-Est et Paris Diderot, 61, Av. du Général de Gaulle, 94010 Créteil Cedex, France*

(Received 11 December 2012; accepted 11 January 2013; published online 31 January 2013)

Highly correlated *ab initio* calculations (CCSD(T)) are used to compute gas phase spectroscopic parameters of three isotopologues of the methyl acetate (CH_3COOCH_3, CD_3COOCH_3, and CH_3COOCD_3), searching to help experimental assignments and astrophysical detections. The molecule shows two conformers *cis* and *trans* separated by a barrier of 4457 cm^{-1}. The potential energy surface presents 18 minima that intertransform through three internal rotation motions. To analyze the far infrared spectrum at low temperatures, a three-dimensional Hamiltonian is solved variationally. The two methyl torsion barriers are calculated to be 99.2 cm^{-1} (C–CH_3) and 413.1 cm^{-1} (O–CH_3), for the *cis*-conformer. The three fundamental torsional band centers of CH_3COOCH_3 are predicted to lie at 63.7 cm^{-1} (C–CH_3), 136.1 cm^{-1} (O–CH_3), and 175.8 cm^{-1} (C–O torsion) providing torsional state separations. For the 27 vibrational modes, anharmonic fundamentals and rovibrational parameters are provided. Computed parameters are compared with those fitted using experimental data. © *2013 American Institute of Physics*. [http://dx.doi.org/10.1063/1.4789413]

INTRODUCTION

Methyl acetate (MeOAc, CH_3COOCH_3) is a flammable liquid occasionally used as a solvent because of the low toxicity and fast evaporation rate. It is useful as the fast-evaporating component in high-low solvent systems of several polymers and resins.[1] In gas phase, it represents a relevant prebiotic astrophysical molecule for which eventual detection can be expected given the capability of the new ALMA observatory.

To our knowledge, gas phase experimental studies of MeOAc as well as quantum chemical studies of the isolated species are not very frequent.[2–11] Although, methyl acetate has not been already detected in astrophysical sources, new spectroscopic studies have been motivated by the setup of new radioastronomical observatories.[3] The presence of MeOAc in gas phase astrophysical sources was postulated because related molecules such as methyl formate, acetic acid, and many other organic compounds containing methyl groups are listed as astrochemical species. MeOAc could be possibly synthesized through multiple reaction pathways from molecules already detected in hot cores, most notably from acetic acid and methanol.[2] MeOAc lines can contribute to the spectral confusion in hot core surveys.[2]

From 1956, the gas phase infrared and microwave spectra of methyl acetate have been measured.[4–10] Structure and harmonic frequencies have also been calculated using *ab initio* methods.[3,4,11] MeOAc shows two conformers *cis* and *trans* (which refer to the direction of the MeO bond with respect to the C=O double bond), predicted to be different in energy (ΔH^e ~8.5 Kcal/mol ~2970 cm^{-1} in Ref. 10), that can interconvert through the torsion of the C–O single bond of the Ac group. In principle, because the corresponding torsional barrier is relatively high (~4500 cm^{-1}), the analysis of the vibrational spectra of the most stable *cis*-conformer at low temperatures seems to be possible neglecting conformer intertransformation. Even in this more favourable case, the spectral analysis is arduous because the molecule shows two additional internal motions which are the torsions of the two methyl groups that confer non-rigid properties. They each interconvert nine minima of the potential energy surface. The corresponding torsional energy levels are very low and could be populated at the low temperatures of the hot cores. To help astronomical survey analysis, at least two-dimensional models considering the non-rigidity are necessary.[3]

Recently, Tudorie *et al.*[3] have performed a fit of more than 800 microwave and millimeter-wave transitions of *cis*-methyl acetate using the code BELGI-Cs-2Tops developed by Kleiner[3] for molecules showing two inequivalent methyl rotors and a symmetry plane. This code for two inequivalent internal rotors follows another code for one internal top, BELGI-Cs (with a plane of symmetry) described in Ref. 12. They have determined the barrier heights to be 102 cm^{-1} (C–CH_3 torsion) and 422 cm^{-1} (O–CH_3 torsion). Spectroscopic parameters calculated using second order perturbation theory developed for semi-rigid systems and a MP2/6-311++G**

[a)]Author to whom correspondence should be addressed. Electronic mail: senent@iem.cfmac.csic.es.
[b)]Doctora Vinculada al IEM-CSIC; E-mail: rosa.dominguez@upm.es.
[c)]E-mail: miguel.carvajal@dfa.uhu.es.
[d)]E-mail: isabelle.kleiner@lisa.u-pec.fr.

anharmonic force field are in a good agreement with the fitting parameters.[3] The BELGI-Cs-2Tops code[3] has been also employed to help the analysis of the high-resolution infrared spectrum in the C=O stretching region.[4]

In the present paper, highly correlated *ab initio* methods are used to determine as many spectroscopic parameters as possible searching to help experimental assignments. To determine low energy levels of three isotopologues, CH_3COOCH_3, CD_3COOCH_3, and CH_3COOCD_3, for which experimental data are available,[3,5] we solve variationally a three-dimensional Hamiltonian whose independent coordinates are the two torsional C–CH_3 and O–CH_3 angles plus the C–O torsional degree of freedom. This latter coordinate is essential in any model that attempts to describe excited states of each CH_3 top because of the proximity in energy of the three torsional fundamentals. Therefore, this model allows us to discuss previous assignments and to evaluate the effect of interactions between the central bond torsion and the methyl torsions. For these purposes, we have computed equilibrium structures and a three-dimensional potential energy surface. Symmetry considerations are taken into consideration to reduce computational expenses and for labeling the torsional levels. Since methyl acetate has same symmetry properties than ethyl-methyl-ether, we have used various subroutines recently developed.[13,14] Our previous studies of molecules with methyl groups (acetic acid,[15] glicolaldehyde,[16] methyl formate,[17,18] methanol,[19] and dimethyl ether[20,21]) are employed in the discussion of this paper.

COMPUTATIONAL DETAILS

Electronic structure calculations

All the electronic structure calculations have been performed with GAUSSIAN 09.[22] Molecular geometries have been optimized using MP2 (second order Möller-Plesset theory) and CCSD (coupled cluster using both single and double substitutions).[23] CCSD(T) single point calculations (CCSD + triple excitations added non-iteratively[24]) have been achieved on the CCSD geometries to obtain more accurate energies. The Dunning's correlation consistent basis set cc-pVTZ has been employed in all the calculations.[25]

For the 27 vibrational modes, harmonic fundamental frequencies have been computed from MP2 and CCSD force fields. Anharmonic band centers are also determined from an MP2 anharmonic force field using second order perturbation theory and the algorithms implemented in GAUSSIAN 09.[22]

For the three torsional modes, the energy levels are calculated variationally with the code ENEDIM[26] developed for previous studies of non-rigid molecules.[15–17] Theoretical aspects employed in this code are detailed in Refs. 27–29.

RESULTS AND DISCUSSIONS

The structure of methyl acetate

MeOAc displays two conformers *cis* and *trans* with a plane of symmetry that interconvert through the internal rotation of the C-O single bond. In Tables I–III, their structural parameters, total electronic energies, relative energies, rotational constants, dipole moments, and torsional barriers are shown. Figure 1 displays the two conformer interconversion process and Figure 2 represents the most stable *cis*-MeOAc structure and the three torsional coordinates α (C–O torsion) and θ_1 and θ_2 (methyl group torsions). In both conformers, one of the hydrogen atoms of each methyl group lies in the molecular symmetry plane. The α coordinate can be identified with the β = C5O3C1C4 dihedral angle ($\alpha = \beta - 180^\circ$). Both conformers are asymmetric tops. The more asymmetric structure, the *trans*-, shows a significant dipole moment.

TABLE I. CCSD and CCSD(T) total electronic energies (E, in a.u.) and relative energies (E_r, in cm^{-1}), CCSD/cc-pVTZ structural parameters, and rotational constants (in MHz) and dipole moments (μ in debye) of *cis*-methyl acetate. The numbering of the atoms is specified in Figure 2.

$\alpha = 0.0^\circ$	$A_e = 10303.6279$
$\theta_1 = 0.0^\circ$	$B_e = 4210.8384$
$\theta_2 = 0.0^\circ$	$C_e = 3104.3979$
E = −267.935357 (CCSD)	$\mu = 1.9973$
E = −267.976500 (CCSD(T))	$\mu_a = 1.9774$
$E_r = 0.0$	$\mu_b = 0.2809$
	$\mu_c = 0.0$

Bond distances (in Å)		Planar angles (in deg)	
O2C1	1.2027	O3C1O2	123.5
O3C1	1.3448	C4C1O3	110.9
C4C1	1.5030	C5O3C1	114.5
C5O3	1.43	H6C4C1	109.5
H6C4	1.0848	H7C4C1=H8C4C1	109.7
H7C4=H8C4	1.0889	H9C5O3	105.7
H9C5	1.0851	H10C5O3=H11C5O3	110.6
H10C5=H11C5	1.0876		
Dihedral angles (in deg)			
C5O3C1C4	180.0	H9C5O3C1	180.0
H6C4C1O3	180.0	H10C5O3H9	119.6
H7C4C1H6	121.0	H11C5O3H9	− 119.6
H8C4C1H6	− 121.0		

The CCSD(T) energy difference between the *cis* and *trans* geometries has been computed to be $\Delta H^e = 2723\ cm^{-1}$. If the harmonic zero point vibrational energy (ZPVE) is taken into consideration, we obtain $\Delta H^e = 2604.2\ cm^{-1}$, $\Delta H^e = 2604.0\ cm^{-1}$, and $\Delta H^e = 2605.1\ cm^{-1}$ for the three isotopologues CH_3–$COOCH_3$, CD_3–$COOCH_3$, and CH_3–$COOCD_3$, respectively. The *cis* → *trans* process transition state is placed at $\alpha = 93^\circ$ and at ∼4500 cm^{-1} over the most stable geometry (see Table III and Figure 1). The transformation is accompanied by slight variations of 0.01 Å of the lengths of the C–C and C–O bonds and significant changes of the planar and dihedral angles. The behavior of MeOAc is comparable to the methyl formate case for which it was found two conformers *cis* and *trans* for which $\Delta H^e = 1854\ cm^{-1}$ and the *cis* → *trans* barrier height $V = 4826\ cm^{-1}$.[17] Although ΔH^e is relatively high, *trans*-methyl formate has been experimentally observed and tentatively detected in Sagittarius B2(N).[30]

The two methyl torsional coordinates θ_1 (C–CH_3) and θ_2 (O–CH_3) are defined using six dihedral angles β_{11} = H6C4C1O3, β_{12} = H7C4C1O3, β_{13} = H8C4C1O3, and β_{21} = H9C5O3C1, β_{22} = H10C5O3C1, β_{23} = H11C5O3C1

TABLE II. CCSD and CCSD(T) total electronic energies (E, in a.u.) and relative energies (E_r, in cm^{-1}), CCSD/cc−pVTZ structural parameters, and rotational constants (in MHz), dipole moments (μ in debye) and harmonic fundamentals (in cm^{-1}) of trans-methyl acetate. The numbering of the atoms is specified in Figure 2.

$\alpha = 180.0^\circ$	$A_e = 9058.9379$
$\theta_1 = 0.0^\circ$	$B_e = 4437.2657$
$\theta_2 = 0.0^\circ$	$C_e = 3093.6524$
E = −267.922948 (CCSD)	$\mu = 4.9252$
E = −267.964367 (CCSD(T))	$\mu_a = 3.5357$
$E_r = 2723$ (CCSD)	$\mu_b = 3.4287$
$E_r = 2663$ (CCSD)	$\mu_c = 0.0$

Bond distances (in Å)

O2C1	1.1980	O3C1O2	118.9
O3C1	1.3528	C4C1O3	117.8
C4C1	1.5106	C5O3C1	120.0
C5O3	1.4218	H6C4C1	107.9
H6C4	1.0843	H7C4C1=H8C4C1	111.1
H7C4=H8C4	1.0893	H9C5O3	105.7
H9C5	1.0854	H10C5O3=H11C5O3	111.7
H10C5=H11C5	1.0897		

Dihedral angles (in deg)

C5O3C1C4	0.0	H9C5O3C1	180.0
H6C4C1O3	180.0	H10C5O3H9	118.4
H7C4C1H6	120.0	H11C5O3H9	−118.4
H8C4C1H6	−120.0		

CCSD harmonic frequencies

A′				A″			
ν_1	3196	ν_{10}	1312	ν_{18}	3150	ν_{23}	1076
ν_2	3175	ν_{11}	1211	ν_{19}	3134	ν_{24}	586
ν_3	3081	ν_{12}	1145	ν_{20}	1533	ν_{25}	237
ν_4	3063	ν_{13}	1024	ν_{21}	1505	ν_{26}	137
ν_5	1875	ν_{14}	817	ν_{22}	1193	ν_{27}	63
ν_6	1527	ν_{15}	591				
ν_7	1510	ν_{16}	484				
ν_8	1487	ν_{17}	334				
ν_9	1424						

TABLE III. CCSD(T) vibrationally corrected potential energy parameters (in cm^{-1}).[a]

	CH_3–$COOCH_3$		CD_3–$COOCH_3$	CH_3–$COOCD_3$
		cis → *trans* process		
ΔH^e	2604.2		2604.0	2605.1
$V(\alpha = 93^\circ)$	4456.8		4460.7	4464.9
		cis-methyl acetate		
	Calc.	Expt.[3]	Calc.	Calc.
$V_3(C–CH_3)$	99.2	102	96.4	99.7
$V_3(O–CH_3)$	413.1	422	412.3	407.8
V_T	515.2		511.7	510.6
Dif	2.9		3.0	3.1
		trans-methyl acetate		
	Calc.		Calc.	Calc.
$V_3(C–CH_3)$	544.7		533.2	544.1
$V_3(O–CH_3)$	571.5		569.9	561.6
V_T	1445.3		1432.6	1434.9
Dif	329.1		329.5	329.2

[a] $V_3(C–CH_3) = E(\alpha, 180, 0) – E(\alpha, 0, 0)$; $V_3(O–CH_3) = E(\alpha, 0, 180) – E(\alpha, 0, 0)$; $V_T = E(\alpha, 180, 180) – E(\alpha, 0, 0)$; Dif = $V_T – V_3(C–CH_3) – V_3(O–CH_3)$.

following the recommendations of Ref. 29. Thus,

$$\theta_1 = [(\beta_{11} + \beta_{12} + \beta_{13})/3]^\circ - 180.0^\circ \quad \text{and}$$
$$\theta_2 = [(\beta_{21} + \beta_{22} + \beta_{23})/3]^\circ - 180.0^\circ.$$

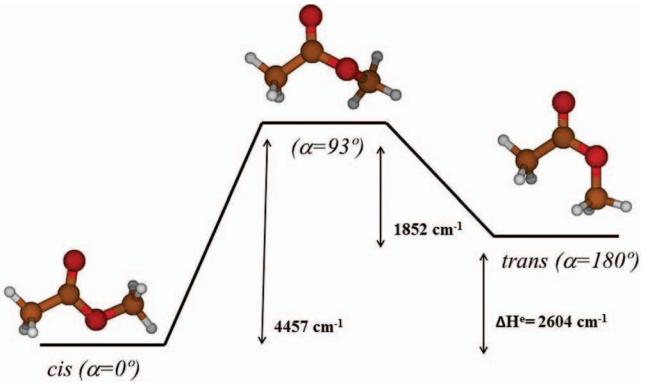

FIG. 1. The *cis*-MeOAc → *trans*-MeOAc interconversion process (the energies are not vibrationally corrected).

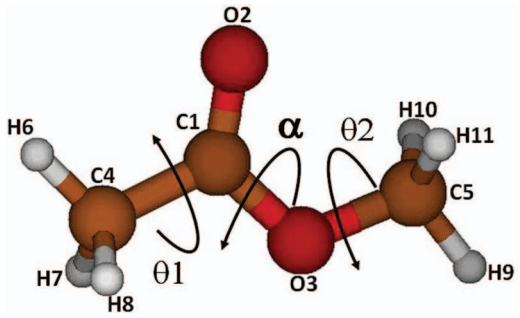

FIG. 2. *cis*-MeOAc at the equilibrium geometry. Definition of the independent coordinates α, θ_1, and θ_2.

The methyl torsional barriers V_3 depend strongly on the α coordinate (see Table III and Figure 3) as well as the methyl interaction terms (see Figure 4). For the most stable *cis*-conformer, they have been determined to be 99.2 cm^{-1} (V_3(C–CH_3)) and 413.1 cm^{-1} (V_3(O–CH_3)) very close to the experimental values of Tudorie *et al.*[3] (102 cm^{-1} and 422 cm^{-1}). For the *trans*-conformer, they were computed to be 544.7 cm^{-1} (V_3(C–CH_3)) and 571.5 cm^{-1} (V_3(O–CH_3)). These parameters can be compared with those of similar molecules. For example, for methyl formate,[17] we have found a larger dependence of V_3(O–CH_3) with α than in MeOAc (V_3(O–CH_3) = 422 cm^{-1} (*cis*) and V_3(O–CH_3) = 9 cm^{-1} (*trans*)). For acetic acid,[15] V_3(C–CH_3) was found to be 169 cm^{-1} and for acetaldehyde[29] to be 392 cm^{-1}, whereas V_3(O–CH_3) was determined to be 378 cm^{-1} for methanol[19] and to be 939 cm^{-1} for dimethyl ether.[20,21]

Therefore, for a realistic determination of the barriers, we have used a flexible model where three curvilinear internal coordinates are frozen, β = C5O3C1C4, β_{11}, and β_{21}, whereas a set of 24 coordinates are allowed to be relaxed. This allows us to take into consideration the interactions between torsions and high and medium frequency vibrational modes.

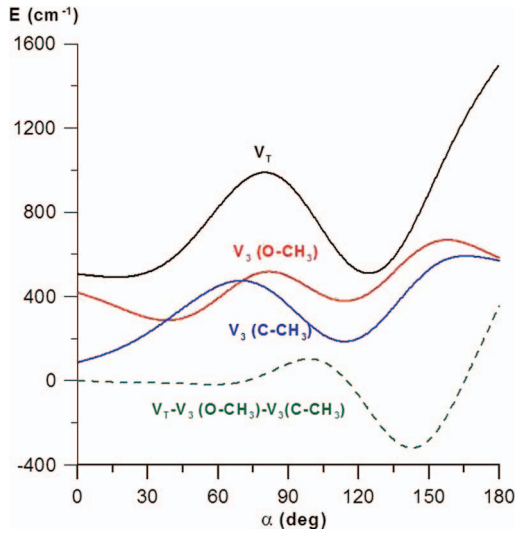

FIG. 3. Evolution of the methyl torsional barriers and the V_T and Dif parameters with the α coordinate. The barriers and parameters can be determined from the total electronic energies with the equations: V_3(C–CH_3) = E(α,180,0) – E(α,0,0); V_3(O–CH_3) = E(α,0,180) – E(α,0,0); V_T = E(α,180,180) – E(α,0,0) and Dif = V_T – V_3(C–CH_3) – V_3(O–CH_3).

Figure 3 shows the evolution of the torsional barriers with the conformer transformation. Barriers are calculated from the total electronic energies with the equations:

$$V_3(C-CH_3) = E(\alpha, 180, 0) - E(\alpha, 0, 0) \text{ and } V_3(O-CH_3) = E(\alpha, 0, 180) - E(\alpha, 0, 0).$$

Two other parameters V_T and Dif defined as: V_T = E(α,180,180) – E(α,0,0) and Dif = V_T – V_3(C–CH_3) – V_3(O–CH_3), are also determined because they depend on the interactions between the two methyl groups. When Dif ~0, as it almost occurs with the *cis*-conformer when the C–O torsion is not highly excited, both methyl groups rotate independently.

Full dimensional anharmonic analysis

Tables II and IV collect the infrared band center positions of *cis*-MeOAc and *trans*-MeOAc derived from the full-dimensional analysis. For the most stable *cis*-conformer, harmonic, and anharmonic fundamental frequencies of three isotopologues have been determined with MP2/cc-pVTZ and harmonic ones at the CCSD/cc-pVTZ level. In Table IV, they are compared with previous experimental data. For the less stable *trans*-MeOAc, only MP2 harmonic frequencies corresponding to the most abundant isotopic variety are shown in Table II.

Calculated frequencies of *cis*-MeOAc are compared with gas phase experimental data from George *et al.*[8] and Shimanouchi.[5] Five modes are predicted to lie below 500 cm^{-1}, three *out-of-plane* vibrations, the C–CH_3 torsion (ν_{27}), the O–CH_3 torsion (ν_{26}), the C–O single bond torsion (ν_{25}), and two *in-plane* bending modes ν_{17} (COC bending) and ν_{16} (CCO bending). Their harmonic frequencies of CH_3–$COOCH_3$ have been found to be 43, 154, 182, 291, and 426 cm^{-1} with MP2/cc-pVTZ and 65, 156, 181, 294, and 431 cm^{-1} with CCSD/cc-pVTZ (Table IV). The MP2

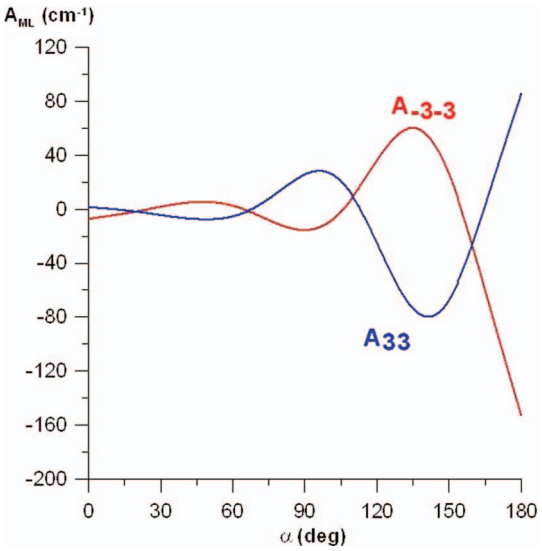

FIG. 4. The A_{33} and A_{-3-3} coefficients corresponding to the cos $3\theta_1$cos $3\theta_2$ and sin $3\theta_1$sin $3\theta_2$ terms of the 2D-potential energy surface evolution with the α coordinate.

TABLE IV. Harmonic (ω) and anharmonic (ν) fundamental frequencies of *cis*-MeOAc (in cm^{-1}).[a]

			CH_3–$COOCH_3$				CD_3–$COOCH_3$			CH_3–$COOCD_3$		
Sym[b]	Mode[c]	Assign.	MP2 (ω)	MP2 (ν)	CCSD (ω)	Expt.[d]	MP2 (ν)	CCSD (ω)	Expt.[e]	MP2 (ν)	CCSD (ω)	Expt.[e]
A′	ν_1	^{C}CH$_3$ st	3225	3080	3195	3028	2310	2369	2275	3080	3195	3031
	ν_2	$^\circ$CH$_3$ st	3222	3083	3188	3028	3083	3188	3032	2315	2368	2288
	ν_3	^{C}CH$_3$ st	3102	2992	3083	2940	2148	2216	2087	2991	3083	2964
	ν_4	$^\circ$CH$_3$ st	3097	3035	3082	2955	3045	3082	2967	2103	2208	2104
	ν_5	C=O st	1809	1780	1856	1747	1774	1853	1768	1776	1855	1769
	ν_6	$^\circ$CH$_3$ b	1521	1504	1525	1455	1503	1525	…	1089	1158	1106
	ν_7	^{C}CH$_3$ b	1490	1452	1501	1438	1039	1073	1086	1447	1494	…
	ν_8	$^\circ$CH$_3$ b	1484	1447	1492	1438	1465	1498	1439	1088	1096	1050
	ν_9	^{C}CH$_3$ b	1406	1371	1426	1372	1011	1052	1007	1371	1430	1375
	ν_{10}	Skel.def.	1291	1246	1318	1249	1262	1335	1268	1269	1332	1268
	ν_{11}	$^\circ$CH$_3$ r	1219	1192	1234	1190	1194	1237	1160	950	976	985
	ν_{12}	O–CH$_3$ st	1096	1063	1114	1051	1089	1133	1049	1024	1051	1043
	ν_{13}	^{C}CH$_3$ r	999	986	1010	982	783	807	780	1069	1082	947
	ν_{14}	Skel.def.	869	849	884	846	863	887	860	790	815	781
	ν_{15}	Skel.def.	651	638	659	638	607	618	599	621	639	619
	ν_{16}	CCO b	426	428	431	433	396	399	390	416	420	420
	ν_{17}	COC b	291	276	294	302	278	280	298	271	272	270
A″	ν_{18}	$^\circ$CH$_3$ st	3189	3049	3160	3002	3049	3160	3004	2290	2346	2263
	ν_{19}	^{C}CH$_3$ st	3186	3055	3154	3002	2281	2334	2253	3054	3154	2994
	ν_{20}	$^\circ$CH$_3$ b	1506	1469	1509	1462	1468	1509	…	1076	1092	1050
	ν_{21}	^{C}CH$_3$ b	1496	1453	1501	1445	1054	1082	1033	1449	1501	…
	ν_{22}	$^\circ$CH$_3$ r	1192	1168	1202	1161	1168	1202	1181	914	932	908
	ν_{23}	^{C}CH$_3$ r	1073	1050	1088	1051	919	950	918	1049	1087	1015
	ν_{24}	C=O w	611	608	621	609	526	537	525	602	618	600
	ν_{25}	Tor	182	178	181	203[f]	172	175	178	164	167	165
	ν_{26}	$^\circ$CH$_3$ T	154	121	156	…	133	155	…	107	116	…
	ν_{27}	^{C}CH$_3$ T	43	76	65	…	53	48	…	75	65	…

[a]*Ab initio* calculations of the harmonic and anharmonic frequencies by using MP2/cc-pVTZ and CCSD/cc-pVTZ levels of theory when indicated MP2 and CCSD, respectively.
[b]Symmetry of the vibrational modes in the Cs symmetry point group.
[c]Assignment given to the vibrational modes: st, stretching; b, bending; r, rocking; T, torsion; w, wagging; skel.Def., skeleton deformation.
[d]Gas phase data from Ref. 8.
[e]Gas phase data from Ref. 5.
[f]Solid state measurement from Ref. 8.

anharmonic fundamentals determined with second order perturbation theory (PT2) considering Fermi displacements are found at 76, 121, 178, 276, and 428 cm^{-1}, for ν_{27}, ν_{26}, ν_{25}, ν_{17}, and ν_{16}, respectively.

In gas phase, experimental data are available for only three low frequency modes: the two bending modes ν_{16} and ν_{17} and the ν_{25} torsion. For the most abundant isotopologue, there is a good agreement between theoretical and experimental data for ν_{16}, whereas ν_{17} and ν_{25} are underestimated. For the medium and high vibrational modes, the agreement is acceptable.

For the methyl group internal rotations, the PT2 model only represents a first approximation given the low torsional barriers. The model allows us to predict some spectroscopic parameters (rotational constants, centrifugal distortion constant,[31] etc.) as those that are shown in Table V and compared with experimental fitted data from Tudorie *et al.*[3]

Although, the PT2 anharmonic analysis is not sufficient for a spectral analysis of a far infrared spectrum, it can be employed to predict interactions between the torsional modes and the remaining vibrational modes and to evaluate the validity of a reduced model in two or three-dimensions. For the isotopologues CH_3–$COOCH_3$ and CD_3–COOCH3, Fermi displacements of the $2\nu_{26}$ are expected given the proximity in energy of the ν_{17} fundamental. The torsional modes ν_{27} and ν_{25} seem to be free of resonances caused by the 24 small amplitude vibrations.

The far infrared spectra (FIR)

To predict far infrared transitions of methyl acetate, we assume the independence of the three torsional modes with respect to the remaining vibrational modes. Thus, the torsional energy levels can be calculated by solving variationally a vibrational Hamiltonian depending on the three curvilinear coordinates α, θ_1, and θ_2:[14,15,27–29]

$$\mathcal{H}(\alpha,\theta_1,\theta_2) = -\sum_{i=1}^{3}\sum_{j=1}^{3} Bq_iq_j(\alpha,\theta_1,\theta_2) + V(\alpha,\theta_1,\theta_2) + V'(\alpha,\theta_1,\theta_2) + V^{ZPVE}(\alpha,\theta_1,\theta_2), \quad q_i, q_j = \alpha,\theta_1,\theta_2. \tag{1}$$

TABLE V. Predicted spectroscopic properties (in cm^{-1})[a] of *cis*-methyl acetate and some of their deuterated isotopologues using second order perturbation theory calculated with MP2/cc-pVTZ.

	CH_3–$COOCH_3$		CD_3–$COOCH_3$	CH_3–-$COOCD_3$
	Calc.	Expt.[3b]	Calc.	Calc.
A_e	0.340682		0.312864	0.321545
B_e	0.140789		0.125401	0.124536
C_e	0.103443		0.094199	0.094497
A_0	0.339180	0.34115(1)	0.311207	0.319964
B_0	0.139085	0.138914(2)	0.123999	0.123164
C_0	0.102405	0.102507(2)	0.093316	0.093609
$A(v = 25)$	0.339446		0.309926	0.318557
$B(v = 25)$	0.138454		0.123841	0.123014
$C(v = 25)$	0.102119		0.093454	0.093750
$A(v = 26)$	0.337617		0.311336	0.320127
$B(v = 26)$	0.138874		0.123530	0.122714
$C(v = 26)$	0.102559		0.093094	0.093417
$A(v = 27)$	0.340749		0.312269	0.321334
$B(v = 27)$	0.138644		0.123619	0.122826
$C(v = 27)$	0.102409		0.093348	0.093603
κ	−0.6852		−0.7146	−0.7354
ΔJ	0.26482×10^{-7}		0.18711×10^{-7}	0.21000×10^{-7}
ΔJK	0.1808×10^{-6}		0.3623×10^{-6}	0.5138×10^{-7}
ΔK	0.7151×10^{-7}		-0.1504×10^{-6}	0.1505×10^{-6}
δJ	0.7612×10^{-8}		0.4909×10^{-8}	0.5491×10^{-8}
δK	-0.6825×10^{-7}		-0.3075×10^{-7}	-0.5732×10^{-7}
Predicted displacements of the $2\nu_{26}$ overtone and the ν_{17} fundamental by Fermi resonance				
ν_{17}	$267\ cm^{-1} \rightarrow 276\ cm^{-1}$		$267\ cm^{-1} \rightarrow 278\ cm^{-1}$	...
$2\nu_{26}$	$231\ cm^{-1} \rightarrow 222\ cm^{-1}$		$255\ cm^{-1} \rightarrow 244\ cm^{-1}$	...

[a]The predicted centrifugal distortion constants are parameters of the reduced asymmetric Hamiltonian.[31]
[b]The values of the rotational constants are given after transformation into the PAM system.

In Eq. (1), Bq_iq_j represents the kinetic energy parameters that can be identified with the $g_{q_iq_j}$ elements of the G matrix (in cm^{-1}):

$$B_{ij} = 1/2^2 g_{ij}.$$

V, V′ and V^{ZPVE} are the three-dimensional potential energy surface, the pseudopotential and the zero point vibrational energy correction (for the definition of V′ see Refs. 27 and 28). They can be determined from the energies, geometries, and harmonic frequencies, respectively.

All the parameters of the 3D-Hamiltonian can be determined accurately using highly correlated *ab initio* methods. For this purpose, we have selected a grid of 148 geometries defined for a set of discrete values of the dihedral angles C5O3C1C4 (180°, 160°, ..., 20°, 0°), H6C4C1O3 (180°, 90°, 0°, −90°), and H9C5O3C1 (180°, 90°, 0°, −90°). The grid has been chosen following the recommendations of Smeyers and Villa.[32] The 148 geometries are partially optimized with CCSD/cc-pVTZ where the remaining 24 coordinates are allowed to be relaxed in order to consider partially the vibrational interactions of the three torsional modes under study with the neglected 24 modes. Besides, the energies are refined performing single points CCSD(T)/cc-pVTZ calculations.

The 3D-potential energy surface, $V(\alpha, \theta_1, \theta_2)$ (3D-PES), has been determined through the fitting of the 148 CCSD(T) energies to a symmetry adapted series which bear the totally symmetric representation of the Molecular Symmetry Group (MSG). CH_3–$COOCH_3$ as well as the two isotopologues CD_3–$COOCH_3$ and CH_3–$COOCD_3$ can be classified in the C_s point group and in the G_{18} MSG (see the Appendix, Table I in Ref. 33, and Ref. 34). The analytical form of the 3D-PES can be

$$V(\alpha, \theta_1, \theta_2) = \sum_{N=0}^{9}\sum_{M=0}^{2}\sum_{L=0}^{2} A_{N3M3L}\cos(N\alpha)\cos(3M\theta_1)\cos(3L\theta_2) + \sum_{N=0}^{9} A_{N-3-3}\cos(N\alpha)\sin(3\theta_1)\sin(3\theta_2)$$

$$+\sum_{N=1}^{8}\sum_{M=0}^{2} A_{-N3M-3}\sin(N\alpha)\cos(3M\theta_1)\sin(3\theta_2)$$

$$+\sum_{N=1}^{8}\sum_{L=0}^{2} A_{-N-33}\sin(N\alpha)\sin(3\theta_1)\cos(3L\theta_2), \quad (2)$$

$V(\alpha, \theta_1, \theta_2)$ is the only Hamiltonian term in Eq. (1) that is isotopically invariant. See supplementary material where the computed 148 expansion coefficients A_{NML} are provided.[35] The pseudopotential V´ as well as the B_{qiqj} depend on the isotopic substitution. For each isotopologue and geometry, they can be calculated using the subroutine MATRIZG[27,28] implemented in the code ENEDIM[26] and fitted to equations formally identical to Eq. (2). For MeOAc, V′ is negligible in all the conformations and the kinetic parameters vary very slightly with the torsions. Their values (in cm^{-1}) for $\alpha = 0^\circ$, $\theta_1 = 0^\circ$, and $\theta_2 = 0^\circ$ are:

	$B_{\alpha\alpha}$	$B_{\theta 1\theta 1}$	$B_{\theta 2\theta 2}$	$B_{\alpha\theta 1}$	$B_{\alpha\theta 2}$	$B_{\theta 1\theta 2}$
$CH_3-COOCH_3$	1.7593	5.7193	6.3011	−0.365	−1.0801	0.5625
$CD_3-COOCH_3$	1.6655	3.0644	6.2845	−0.3497	−1.0408	0.5597
$CH_3-COOCD_3$	1.3609	5.6888	3.1903	−0.2484	−0.5169	0.4349

$V^{ZPVE}(\alpha, \theta_1, \theta_2)$ represents a correction of the 3D-PES that usually shifts the torsional levels an amount of ∼5 cm^{-1}. With this correction, the contribution of the 24 neglected modes to the vibrational energy is taken into consideration. Otherwise, it is considered to be equal to zero since the geometry optimization minimizes it. For each isotopologue and for each MP2 geometry, $V^{ZPVE}(\alpha, \theta_1, \theta_2)$ is determined from the MP2/aug-cc-pVTZ harmonic frequencies ω_i:

$$E^{ZPVE} = \sum_{i=n+1}^{i=3N-6} \frac{\omega_i}{2}, \quad (3)$$

where n is equal to the number of independent coordinates, the three torsional modes in the case of methyl acetate in this paper. The sum starts with n + 1 because their contribution to the vibrational energy is considered explicitly in the variational calculations. Individual values of the ZPVE correction corresponding to the 148 conformations are fitted to totally symmetric series formally identical to Eq. (2).

The Hamiltonian was solved variationally using as trial functions symmetry eigenvectors corresponding to the G_{18} MSG. An acceptable numerical convergence requires 65 × 39 × 39 basis functions. The symmetry properties factorize the Hamiltonian matrix into blocks whose dimensions are 5493 (A_1) 5492 (A_2) and 10 985 (E_1, E_2, E_3, E_4, E_3, E_4). Large matrices are pre-diagonalized using contracted basis sets since solutions of a one-dimensional Hamiltonian depending on α are multiplied by symmetry eigenvectors depending on θ_1 and θ_2, to produce the trial function.

In Tables VI–VIII, the computed torsional energy levels and the FIR frequencies are shown for MeOAc and some of their deuterated isotopologues. In Table VI, the tunneling splittings of the levels that could be populated at low temperatures are also shown. All the energies are referred to the $(vv'v'') = (000)$ ground state and are labeled using the G_{18} symmetry group and three vibrational quanta v, v′, and v″ corresponding to the ν_{25}, ν_{27}, and ν_{26} modes. All of them are assigned to the *cis*-conformer because they are lying below ΔH^e (∼2600 cm^{-1}).

Below ΔH^e, each *cis* energy level splits into five components (A_i (i = 1,2), E_1, E_2, E_3, E_4) (see Table VI), with degeneracies accounting for nine wave functions, because the *cis* conformer local potential energy surface presents nine minima derived from the two internal rotations of the methyl groups. The C–CH_3 first excited level (010) lies below the V_3(C–CH_3) barrier (∼100 cm^{-1}, see Table III), whereas (020) reaches the barrier top. Internal rotation splittings between A and E levels reach 11.81 cm^{-1} in the (010) state and 26.42 cm^{-1} in the (020) state for the most abundant isotopologue (they are 2.21 cm^{-1} and 9.41 cm^{-1} in CD_3–$COOCH_3$ and 11.59 cm^{-1} and 26.7 cm^{-1} in CH_3–$COOCD_3$). For the CH_3–$COOCH_3$ main species, the computed torsional splittings in the vt = 0 ground torsional state (000) agree very well with the values inferred from the experimental microwave data using the BELGI-Cs-2Tops code, which are 1.15 cm^{-1} for the A-E_1 splitting, 0.01 cm^{-1} for the A-E_2 and 1.16 cm^{-1} for the A-E_3 and A-E_4 splittings.[3]

For the O–CH_3, the barrier height is ∼410 cm^{-1}. In this case, the first excited level (001) lies in the bottom of the well. Internal rotation splittings between A and E species are predicted to be 2.26 cm^{-1} for CH_3–$COOCH_3$, 2.55 cm^{-1} for CD_3–$COOCH_3$ and 0.34 cm^{-1} for CH_3–$COOCD_3$.

It is expected that some vibrational energies around 300 cm^{-1} and around 430 cm^{-1} in Table VI would interact strongly with ν_{17} and ν_{16} bands, respectively, due to their proximity in energy and, hence, their vibrational term values could be slightly different from those presented in this work. A more general procedure should be used in order to solve these possible energy shifts although this is out of the aim of this work.

FIR band centers for the three isotopologues are shown in Table VII. The three fundamental frequencies 000 → 100 (ν_{25}), 000 → 010 (ν_{27}), and 000 → 001 (ν_{26}) have been determined to be 175.8 cm^{-1}, 63.7 cm^{-1}, and 136.1 cm^{-1} (CH_3–$COOCH_3$), 171.5 cm^{-1}, 43.9 cm^{-1}, and 132.9 cm^{-1} (CD_3–$COOCH_3$) and 151.4 cm^{-1}, 63.0 cm^{-1}, and 105.5 cm^{-1} (CH_3–$COOCD_3$). For ν_{25}, these fundamentals can be compared with previous experimental frequencies (203 cm^{-1} for CH_3–$COOCH_3$[8] and 178 cm^{-1} and 165 cm^{-1}

TABLE VI. Torsional energy levels (in cm^{-1}) of *cis*-MeOAc.

vv′v″	Symm.	CH_3–$COOCH_3$	CD_3–$COOCH_3$	CH_3–$COOCD_3$
000	A_1	0.00[a]	0.00[b]	0.00[c]
	E_1	1.08	0.13	1.08
	E_2	0.01	0.01	0.00
	E_3	1.09	0.13	1.08
	E_4	1.09	0.13	1.08
010	A_2	63.74	43.59	63.03
	E_1	51.93	41.37	51.44
	E_2	63.74	43.60	63.03
	E_3	51.93	41.38	51.44
	E_4	51.93	41.38	51.44
020	A_1	87.35	71.33	86.87
	E_1	113.77	80.74	113.64
	E_2	87.35	71.34	86.87
	E_3	113.77	80.74	113.64
	E_4	113.77	80.74	113.64
001	A_2	136.09	132.88	105.46
	E_1	137.98	135.26	105.79
	E_2	135.72	132.71	105.45
	E_3	136.73	134.91	105.78
	E_4	136.73	134.91	105.78
100	A_2	175.81	171.47	151.39
	E_1	178.62	170.26	149.55
	E_2	175.75	171.39	151.39
	E_3	178.56	170.20	149.55
	E_4	178.56	170.20	149.55
011	A_1	196.9	178.9	167.0
030	A_2	216.9	137.2	219.4
040	A_1	221.5	136.7	232.2
021	A_2	229.4	206.8	190.8
110	A_1	246.5	217.3	206.7
002	A_1	248.0	246.6	199.0
120	A_2	271.9	248.3	249.1
101	A_1	304.5	298.2	255.4
012	A_2	309.5	275.3	259.0
220	A_1	333.0	274.8	283.3
200	A_1	348.6	339.7	301.3
041	A_2	351.9	291.5	335.7
031	A_1	358.6	318.7	323.5
003	A_2	361.7	360.2	281.0
111	A_2	376.6	344.8	309.7
004	A_1	381.8	379.2	326.8
140	A_2	394.1	314.6	353.8
130	A_1	395.8	312.4	369.1
121	A_1	405.1	375.6	351.7
102	A_2	415.0	408.5	348.1
013	A_1	424.3	382.6	345.2
210	A_2	424.6	387.7	386.9
023	A_2	437.8	379.6	363.1
220	A_1	452.5	421.7	406.6
014	A_2	456.6	400.9	395.2
024	A_1	463.0	401.4	417.6
201	A_2	470.9	460.5	404.0
032	A_2	471.8	419.5	416.0
042	A_1	473.3	407.2	432.3
050	A_2	480.9	262.9	478.2
060	A_1	481.0	261.5	478.3
112	A_1	487.6	442.3	401.1
131	A_2	510.3	441.2	443.3
300	A_2	518.9	505.7	449.9
141	A_1	517.7	457.9	455.2
103	A_1	526.0	519.0	494.9

[a]ZPVE = 191.3 cm^{-1}.
[b]ZPVE = 181.1 3 cm^{-1}.
[c]ZPVE = 160.4 3 cm^{-1}.

for CD_3–$COOCH_3$ and CH_3–$COOCD_3$[5]). Unfortunately, for ν_{26} and ν_{27}, there are not direct measures of far infrared bands in gas phase that permit us to evaluate the accuracy of our calculated values. For ν_{25}, there is only a low resolution measurement in the solid phase and again no gas phase measurement so far. It has to be remarked that our PT2 full-dimensional calculations predict Fermi resonances between the $2\nu_{26}$ overtone and the ν_{17} COC bending fundamental which are not considered in our 3D model. Finally we can also compare the *ab initio* values of the FIR 000 → 010 (ν_{27}) and 000 → 001 (ν_{26}) band centers for the main isotopologue to the values extrapolated from our calculation using the BELGI-Cs-2Tops code which are 62.6 cm^{-1} and 133.08 cm^{-1}, respectively.[3] Those values represent only an extrapolation because neither rotational transitions within the first excited torsional states of any top nor far-infrared transitions have been analyzed so far. Nevertheless, they are quite close.

Table VII also shows several sequences between excited torsional levels and combination band centers probably visible at low temperatures. For ν_{25}, 100 → 200 and 200

TABLE VII. Far infrared transitions (in cm^{-1}) connecting *cis*-methyl acetate non-degenerate levels.

vv′v″ → vv′v″	Symm.	CH_3–$COOCH_3$	CD_3–$COOCH_3$	CH_3-$COOCD_3$
000 → 100	$A_1 \rightarrow A_2$	175.8	171.5	151.4
100 → 200	$A_2 \rightarrow A_1$	172.8	168.2	149.9
200 → 300	$A_1 \rightarrow A_2$	170.3	166.0	148.0
000 → 010	$A_1 \rightarrow A_2$	63.7	43.9	63.0
000 → 030	$A_1 \rightarrow A_2$	216.9	137.2	219.4
010 → 020	$A_2 \rightarrow A_1$	22.7	27.4	23.9
010 → 040	$A_2 \rightarrow A_1$	157.8	92.8	169.2
020 → 030	$A_1 \rightarrow A_2$	129.5	65.9	132.5
000 → 001	$A_1 \rightarrow A_2$	136.1	132.9	105.5
001 → 002	$A_2 \rightarrow A_1$	111.9	113.7	93.5
002 → 003	$A_1 \rightarrow A_2$	113.7	113.6	82.0
100 → 110	$A_2 \rightarrow A_1$	70.7	45.8	55.3
010 → 110	$A_2 \rightarrow A_1$	182.8	173.5	143.7
020 → 120	$A_1 \rightarrow A_2$	184.5	177.0	162.2
100 → 101	$A_2 \rightarrow A_1$	128.7	126.7	104.0
001 → 101	$A_2 \rightarrow A_1$	168.4	165.3	149.9
001 → 011	$A_2 \rightarrow A_1$	60.8	46.0	61.5
010 → 011	$A_2 \rightarrow A_1$	133.2	135.1	104.0
020 → 021	$A_1 \rightarrow A_2$	142.0	135.5	103.9
110 → 111	$A_1 \rightarrow A_2$	130.1	127.5	103.0
120 → 121	$A_2 \rightarrow A_1$	132.2	127.3	102.6
101 → 111	$A_1 \rightarrow A_2$	72.1	46.6	54.3
011 → 111	$A_1 \rightarrow A_2$	179.7	165.9	142.7
021 → 121	$A_2 \rightarrow A_1$	175.7	168.8	160.9

→ 300, determined at 172.8 cm^{-1} and 170.3 cm^{-1} for the most abundant isotopologue, present a standard anharmonic behavior. However, the methyl torsional barriers (102 cm^{-1} and 422 cm^{-1},[3]) are rather low making really hard the labeling of the levels.

A comparison between theoretical models and experimental data

Usually, the large amplitude vibrations of two methyl group systems are analyzed using two-dimensional effective Hamiltonians depending on the two internal rotations. Recently, Tudorie *et al.*[3] have developed a fitting program for the analysis of the microwave and millimeter-wave spectra of molecules with two inequivalent methyl tops and a symmetry plane such as MeOAc. To compare our new *ab initio* results with the available fitted parameters,[3] we have reduced our 3D-PES[35] to obtain a 2D-surface,[21] by freezing the α coordinate at 0°. Then, we obtain

$$\begin{aligned} V(\theta_1,\theta_2) = {} & 269.642 - 206.919\,cos3\theta_2 - 13.447\,\cos 6\theta_2 \\ & - 50.081\,\cos 3\theta_1 + 0.707\,\cos\,3\theta_1 \cos 3\theta_2 \\ & - 0.227\,\cos 3\theta_1 \cos 6\theta_2 + 0.548\,\cos 6\theta_1 \\ & - 0.36\,\cos 6\theta_1 \cos 3\theta_2 + 0.112\,\cos 6\theta_1 \cos 6\theta_2 \\ & + 6.489\,\sin 3\theta_1 \sin 3\theta_2. \end{aligned} \quad (4)$$

In Table VIII, the energy levels calculated from this 2D-PES are shown. For this purpose, we have used the kinetic parameters, $B_{\theta 1\theta 1} = 5.66\ cm^{-1}$, $B_{\theta 1\theta 2} = 0.34\ cm^{-1}$, and $B_{\theta 2\theta 2} = 5.64\ cm^{-1}$ determined in two-dimensions with MATRIZ G[26,27] from the CCSD/cc-pVTZ equilibrium geometry. Furthermore, the 2D-PES is reduced for obtaining energies with 1D-Hamiltonians involving only either θ_1 or θ_2 degrees of freedom following the same procedure.

Our 2D-PES compares well with the one of Tudorie *et al.*,[3] fitted using experimental data:

$$\begin{aligned} V(\theta_1,\theta_2) = {} & 258.418 - 207.548\,\cos 3\theta_2 - 47.344\,\cos 3\theta_1 \\ & - 3.526\,\cos 3\theta_1 \cos 3\theta_2 + 34.24\,\sin 3\theta_1 \sin 3\theta_2. \end{aligned} \quad (5)$$

TABLE VIII. Non-degenerate torsional energy levels (in cm^{-1}) calculated with different reduced models.

Model		3D[a]	2D[b]	1D[c]	1D[d]	2D[3]
Independent variables		$\alpha, \theta_1, \theta_2$	θ_1, θ_2	θ_1	θ_2	θ_1, θ_2
$vv'v''$	Symmetry					
000	A_1	0.0[a]	0.0[b]	0.0[c]	0.0[d]	0.0[e]
010	A_2	63.7	64.9	65.1	…	62.6
020	A_1	87.4	83.5	83.7	…	83.1
001	A_2	136.1	141.2	…	140.7	133.1
100	A_2	175.8	…	…	…	…
011	A_1	196.9	205.4	…	…	189.4
030	A_2	216.9	221.1	223.0	…	205.6
040	A_1	221.5	223.4	223.2	…	222.5
021	A_2	229.4	226.2	…	…	226.6

[a]ZPVE = 191.4 cm^{-1}.
[b]ZPVE = 107.0 cm^{-1}.
[c]ZPVE = 30.8 cm^{-1}.
[d]ZPVE = 76.0 cm^{-1}.

The corresponding levels (last column of Table VIII) were determined using the kinetic parameters of Tudorie *et al.*[3]: $F_1 = 5.554669\ cm^{-1}$ ($F_1 = B_{\theta 1\theta 1}$); $F_{12} = 0.664\ cm^{-1}$ ($F_{12} = 2\,B_{\theta 1\theta 2}$); $F_2 = 5.523464\ cm^{-1}$ ($F_2 = B_{\theta 2\theta 2}$), computed by a least-squares fitting through BELGI-Cs-2Tops code and choosing, as a starting point in the fitting procedure, the values determined from the MP2/6-311++G** equilibrium geometry (see Table VII of Ref. 3). All the energies listed on the last column of Table VII are for A species and for J = K = 0 energy levels, and since there is so far no experimental data for excited torsional states in methyl acetate, these energies represent only extrapolations using the molecular parameters determined from the $v_t = 0$ fit.

With the exception of the $\sin 3\theta_1 \sin 3\theta_2$ term coefficient (A_{0-3-3}), the good agreement between the two surfaces (Eq. (4) and (5)) and the kinetic parameters is evident. These two equations contain a different number of terms because the number of fitted coefficients was restricted by the set of available experimental lines that correspond to transitions involving a limited number of vibrational states. The *ab initio* calculations of this work predict values of the V_6 coefficients of the $\cos 6\theta_i$ terms that are not negligible (V_6(C–CH_3) = 0.548 cm^{-1}, V_6(O–CH_3) = −13.447 cm^{-1}), which justify energy differences for the higher excited states. For further spectral analysis involving excited torsional states, it will be very useful to employ the *ab initio* V_6 parameters as starting point for the fitting procedure.

Differences for other terms are very small. For example, A_{033} differs ∼4 cm^{-1} but these differences can be related to the number of expansion terms, i.e., the coefficients A_{063} and A_{036} are different than zero in the *ab initio* potential surface while they are fixed to zero in the fitted potential surface.

Differences between the A_{0-3-3} terms of Eq. (4) and (5) can be correlated to the interactions between the O–CH_3 torsion and the C–O torsion (modes ν_{26} and ν_{25}). A_{0-3-3}, as well as $B_{\theta 1\theta 2}$, is responsible for the difference between the two methyl torsion fundamentals. Whereas Eq. (4) provides (010) = 64.9 cm^{-1} and (001) = 141.2 cm^{-1}, the levels determined using Eq. (5) are (010) = 62.6 cm^{-1} and (001) = 133.1 cm^{-1}. A good agreement for (010) is obtained whereas (001) differs. However, the 3D energies, that retain the ν_{25} and ν_{26} interactions, ((010) = 63.7 cm^{-1} and (001) = 136.1 cm^{-1}), are in a good agreement with the empirical results. Apart from that difference, differences among *ab initio* energies calculated with the 3D, 2D and 1D models are not important. It can be inferred that the three torsional modes are "almost independent" although, especially for high energies where resonances are more significant, the 3D-model results are the most reliable.

CONCLUSIONS

Highly correlated *ab initio* calculations have been used to compute gas phase spectroscopic parameters of CH_3COOCH_3, CD_3COOCH_3, and CH_3COOCD_3. MeOAc shows two conformers *cis* and *trans* separated by a barrier of 4457 cm^{-1}. Their energy difference ΔH^e has been predicted to be ∼2600 cm^{-1}. To analyze the far infrared spectrum at low temperatures, a 3D-Hamiltonian is solved variationally. The

two methyl torsion barriers are calculated to be 99.2 cm^{-1} (C–CH_3) and 413.1 cm^{-1} (O–CH_3) in a good agreement with available experimental data. The three fundamental torsional band centers of CH_3COOCH_3 are predicted to lie at 63.7 cm^{-1} (C–CH_3), 136.1 cm^{-1} (O–CH_3), and 175.8 cm^{-1} (C–O torsion) providing torsional state separations. These are relatively large for the first excited levels assigned to the C–CH_3 torsion.

Differences between energies calculated with the 3D-model and 2D- and 1D-reduced models are not relevant. It can be inferred that the three torsional modes are "almost independent" although, especially for high energies where resonances are more significant, the 3D-model results are the most believable. In general, the agreement between the present pure *ab initio* results and previous fitted parameters determined using an effective Hamiltonian is evident. For further analysis involving excited torsional states, it is recommendable to use the V_6 *ab initio* coefficients as starting point for further fittings.

ACKNOWLEDGMENTS

This work has been supported by the *Ministerio de Economía y Competividad* of Spain, through Grant Nos. AYA2008-00446 (Plan Nacional I + D + I (2004–2007)) and FIS2011-28738-C02-02, and computing resources of CESGA. Also this work is partly supported by a joint project within the framework of a CNRS (France) and CSIC (Spain) agreement (Code No.: 2011 FR0018). I.K. acknowledge the financial support provided by ANR-08-BLAN-0054 and the support provided by the French PCMI (Programme National de Physique Chimie du Milieu Interstellaire).

APPENDIX: CHARACTER TABLE OF THE G_{18} GROUP[33]

	E	2(456)	2(123)	2(123)(456)	2(123)(465)	9(23)(56)*	$C_3^1xC_3^2$
A_1	1	1	1	1	1	1	AA
A_2	1	1	1	1	1	−1	AA
E_1	2	2	−1	−1	−1	0	EA
E_2	2	−1	2	−1	−1	0	AE
E_3	2	−1	−1	2	−1	0	EE
E_4	2	−1	−1	−1	2	0	EE

[1] A. Siporska and J. Szydlowski, Macromolecules **41**, 4534 (2008).
[2] M. J. Kelley and G. A. Blake, *RCO4, 61st OSU International Sympossium on Molecular Spectroscopy*, Columbus, OH, 2006.
[3] M. Tudorie, I. Kleiner, J. T. Hougen, S. Melandri, L. W. Sutikdja, and W. Stahl, J. Mol. Spectrosc. **269**, 211 (2011).
[4] F. X. Sunahori, N. Borho, X. Liu, and Y. Xu, J. Chem. Phys. **135**, 234310 (2011).
[5] T. Shimanouchi, *Tables of Molecular Vibrational Frequencies Consolidated* (National Bureau of Standards, 1972), Vol. I, pp. 1–160.
[6] B. Nolin and N. Jones, Can. J. Chem. **34**, 1382 (1956).
[7] J. K. Wilmshurst, J. Mol. Spectrosc. **1**, 201 (1957).
[8] W. O. George, T. E. Houston, and W. C. Harris, Spectrochim. Acta Part A **30**, 1035 (1974).
[9] J. Sheridan, W. Bossert, and A. Bauder, J. Mol. Spectrosc. **80**, 1 (1980).
[10] C. E. Blom and H. H. Günthard, Chem. Phys. Lett. **84**, 267 (1981).
[11] J. Dybal and S. Krimm, J. Mol. Struct. **189**, 383 (1988).
[12] I. Kleiner, M. Godefroid, M. Herman, and A. R. W. McKellar, J. Mol. Spectrosc. **142**, 238 (1990).
[13] M. L. Senent, R. Ruiz, R. Dominguez-Gómez, and M. Villa, J. Chem. Phys. **130**, 064101 (2009).
[14] M. L. Senent, R. Ruiz, M. Villa, and R. Domínguez-Gómez, Chem. Phys. **368**, 87 (2010).
[15] M. L. Senent, Mol. Phys. **99**, 1311 (2001).
[16] M. L. Senent, J. Phys. Chem. A **108**, 6286 (2004).
[17] M. L. Senent, M. Villa, F. J. Meléndez, and R. Domínguez-Gómez, Astrophys. J. **627**, 567 (2005).
[18] M. Carvajal, I. Kleiner, and J. Demaison, Astrophys. J., Suppl. Ser. **190**, 315 (2010).
[19] C. Muñoz-Caro, A. Niño, and M. L. Senent, Chem. Phys. Lett. **273**, 135 (1997).
[20] M. Villa, M. L. Senent, R. Domínguez-Gómez, O. Álvarez-Bajo, and M. Carvajal, J. Phys. Chem. A **115**, 13573 (2011).
[21] M. L. Senent, R. Domínguez-Gómez, M. Carvajal, and M. Villa, J. Phys. Chem. A **116**, 6901 (2012).
[22] M. J. Frisch, G. W. Trucks, H. B. Schlegel *et al.*, GAUSSIAN 09, Revision A.1, Gaussian, Inc., Wallingford, CT, 2009.
[23] G. E. Scuseria and H. F. Schaefer III, J. Chem. Phys. **90**, 3700 (1989).
[24] J. A. Pople, M. Head-Gordon, and K. Raghavachari, J. Chem. Phys. **87**, 5968 (1987).
[25] D. E. Woon and T. H. Dunning, Jr., J. Chem. Phys. **98**, 1358 (1993).
[26] M. L. Senent, ENEDIM, a variational code for non-rigid molecules, 2001, see http://tct1.iem.csic.es/senent/PROGRAMAS.htm.
[27] M. L. Senent, Chem. Phys. Lett. **296**, 299 (1998).
[28] M. L. Senent, J. Mol. Spectrosc. **191**, 265 (1998).
[29] V. Szalay, A. G. Császár, and M. L. Senent, J. Chem. Phys. **117**, 6489 (2002).
[30] J. L. Neill, M. T. Muckle, D. P. Zaleski, A. L. Steber, B. H. Pate, V. Lattanzi, S. Spezzano, M. C. McCarthy, and A. J. Remijan, Astrophys. J. **755**, 143 (2012).
[31] J. K. G. Watson, Mol. Phys. **15**, 479 (1968).
[32] Y. G. Smeyers and M. Villa, Chem. Phys. Lett. **235**, 587 (1995).
[33] N. Ohashi, J. T. Hougen, R. D. Suenram, F. J. Lovas, Y. Kawashima, M. Fujitake, and J. Pyka, J. Mol. Spectrosc. **227**, 28 (2004).
[34] M. Carvajal, O. Alvarez-Bajo, M. L. Senent, R. Domínguez-Gómez, and M. Villa, J. Mol. Spectrosc. **279**, 3 (2012).
[35] See supplementary material at http://dx.doi.org/10.1063/1.4789413 for the computed 148 expansion coefficients A_{NML}.